Stony Brook University

Investigation of Materials Surface Chemistry on Osteoblast Proliferation, Migration and Differentiation

A Thesis Presented

by

Xia Lu

to

The Graduate School

in Partial Fulfillment of the

Requirements

for the Degree of

Master of Science

in

Materials Science and Engineering

Stony Brook University

December 2011

Stony Brook University

The Graduate School

Xia Lu

We, the thesis committee for the above candidate for the

Master of Science degree, hereby recommend

acceptance of this thesis.

Yizhi Meng – Thesis Advisor
Assistant Professor, Department of Materials Science and Engineering

Dilip Gersappe – Second Reader
Associate Professor, Graduate Program Director
Department of Materials Science and Engineering

Yi-Xian Qin – Third Reader
Professor
Department of Biomedical Engineering

This thesis is accepted by the Graduate School

Lawrence Martin
Dean of the Graduate School

Abstract of the Thesis

Investigation of Materials Surface Chemistry on Osteoblast Proliferation, Migration and Differentiation

by

Xia Lu

Master of Science

in

Materials Science and Engineering

Stony Brook University

2011

Osteoporosis, a bone disease caused by the decreased mass and impaired structure of bone, is becoming an increasing threat to the health of the elderly population. To treat and prevent this kind of suffering, understanding of the bone formation and regeneration is of significant importance, during which bone cell-biomaterial interaction plays a critical role, especially osteoblasts. In this work, we report an *in situ* investigation of osteoblast proliferation, migration and differentiation on a series of substrates with variable surface chemistry as a result of coating fabrication. Primary investigation indicated that cells migrated faster on sulfonated polystyrene (SPS)-coated MirrIR slides than uncoated slides but grew slower. Cell elongation results were well consistent with the migration data.

To explain these differences, hydrophilicity of SPS-coated and uncoated slides was measured, which turned out that SPS coating made the slides more hydrophobic. However, to successfully explain the results one challenge is that multiple discrepancies co-exist between SPS-coated and uncoated MirrIR slides, excluding surface chemistry, surface roughness and surface charge, which requires future work focusing on realization of univariate parameter at one time. Final understanding of effects of individual parameter listed above on osteoblast proliferation, migration and differentiation is hopeful to help design new implantable materials for clinical surgery.

Table of Contents

List of Figures

List of Tables

Acknowledgments

Foremost, I would like to express my sincere gratitude to my advisor Prof. Yizhi Meng for the continuous support of my master study and research, for her patience, motivation, enthusiasm, and immense knowledge.

Besides my advisor, I would like to thank the rest of my thesis committee: Prof. Dilip Gersappe, and Prof. Yi-Xian Qin, for their encouragement, insightful comments, and hard questions. My sincere thanks also go to Dr. Erik Muller for offering me the research materials and helping me with the AFM study.

I thank my labmates in Meng Group: Kate Dorst, Chi Zhang, Gaojun Liu, Xin He, Cheng Zhang and Ling Li, for the stimulating discussions, for the sleepless nights and weekends we were working together before deadlines, and for all the fun we have had in the last years. Also I thank my friends in Stony Brook University: Shangmin Xiong, Lina Zhang, Liudi Zhang, Huanhuan Wang, for your friendship and encouragement all the time.

Last but not the least, I would like to thank my wonderful family: my parents Shouhuai Lu and Qingxiong Li, my sister Ling Lu, brother Zhenhua Lu and boyfriend Zengcheng Li, for being my constant support throughout these years.

Chapter One. Introduction

Bone is a type of hard tissue that contributes to the constitution of the skeleton structures inside vertebrates. It has multiple functions, such as protecting the brain, heart, lungs and anchoring muscles, but also can suffer some skeletal disorders, among which one of the more prominent is osteoporosis (Figure 1). As a bone disease in which the mass of bone is decreased and the structural integrity of trabecular bone (spongy structure of bone, Figure 1(a)) is impaired, osteoporosis has been defined based on bone mineral density (BMD) by the World Health Organization (WHO), where BMD is lower than 833 mg/cm^3 using standardized bone density measurements of the total hip. Osteoporosis makes the bone weaker and more likely to fracture. For example, according to an investigation using the WHO criteria, the age-adjusted prevalence of osteoporosis rate at the hip, spine or wrist is 35% among women ≥ 50 years of age and 19% in men ≥ 50 years of age[1]. In order to develop an optimal treatment for all those suffering from this kind of disease, the field of tissue engineering (stated by Langer and Vacanti as "an interdiscriplinary field that applies the principles of engineering and life

sciences toward the development of biological substitutes that restore, maintain or improve tissue function or a whole organ"[2]) has been booming, in particular, the understanding of cell-material interaction due to the association of osteo-inductive factors with implantable materials and the association of osteogenic stem cells with these (hybrid) materials is of crucial significance.

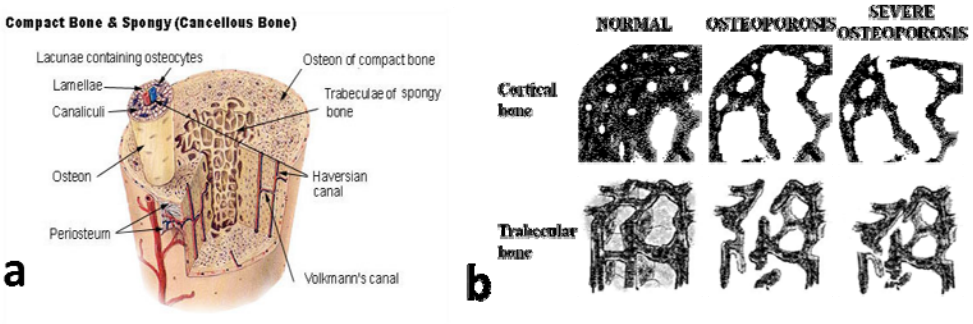

Figure 1 a) Compact Bone and spongy bone: compact (cortical) bone composes the hard outer layer of bones. It has a porosity of 5-30% and gives the smooth, white and solid appearance of bones. This part accounts for 80% of the total bone mass of an adult skeleton, and thus is also referred to as dense bone; trabecular bone (cancellous or spongy bone) is composed of a rod- and plate-like elements, which together form a lighter network with a porosity of 30-90% and allowing room for blood vessels and marrow (training.seer.cancer.gov); b) Schematic view of osteoporosis: when osteoporosis occurs, out layer of cortical bone is reduced and the network of interior trabecular bone is disconnected. This kind of disorder in skeleton could increase if no proper treatment is added and thus accumulate into fracture of bone structure, both in the outer layer and interior. (courses.washington.edu)

As a type of mature bone cells that are responsible for bone formation, osteoblasts arise from osteoprogenitor cells located in the deeper layer of periosteum (a membrane lining the outer surface of all bones, except at the joints of long bones that their length is bigger than the width) and the bone marrow.

They produce osteoid composed of proteins and mineralize the osteoid matrix by depositing minerals of calcium, zinc, copper and sodium etc. Once extracted and cultured *in vitro* (performed not in a living organism but in a controlled environment), osteoblasts will be exposed to substrates that are significantly different from those they encounter *in vivo*, introducing the necessity of understanding the effects of different substrate properties on osteoblast behaviors, such as proliferation, migration and differentiation, which all play significant roles in processes like embryonic development and wound healing.

The cellular response of osteoblasts to biomaterials is modulated by cell adhesion phenomena. Signals generated during the adhesion processes can be transmitted via the transmembrane receptors, to the cytoplasm, to the cytoskeleton and finally to the nucleus, resulting in different consequences in cell behaviors[3]. Therefore, as the early-stage of osteoblast-biomaterial interaction, osteoblast adhesion really indicates the biomaterial's biocompatibility, exhibited by capacities of osteoblasts to proliferate, migrate and differentiate[4]. Investigation of osteoblast-material interactions has revealed the central role of extracellular matrix (ECM)-mediated adhesion, during which focal contacts of cells, an entirety of structural proteins and enzymes first identified in 1971[5], interact with the interface. An important ECM protein fibronectin (Fn), is precipitated from surrounding cell culture media with conditional conformation determined by substrate nature. When the substrate is exposed to media, functional groups

present on the surface can attract soluble proteins in media through chemical or physical interaction and a thin layer of Fn together with other possible proteins sometimes can be deposited. As reported by previous studies, Fn tends to adsorb and form a protein network on more hydrophobic surfaces and in the presence of cells, their adhesion efficiency can be enhanced[6]. On relatively more hydrophilic surfaces, instead, cells may adhere and reorganize adsorbed ECM proteins into a fibril-like pattern [7, 8]. According to those experiments, soluble Fn in media exhibits a globular structure, inner hydrophobic core and outer hydrophilic motifs that results in a stable interaction between Fn molecules and polar solvent molecules. However, after attaching to a substrate, Fn will unfold to a more extended structure, which may then result in the exposure of cryptic binding domains. For example, in cases when arginine-glycine-aspartic acid (RGD) peptide sequence appears, integrin, a type of transmembrane receptors, can bind and thus anchor cells to the substrate surface[9]. The other potential after protein unfolding is that domains for intermolecular interaction appear and contribute to the further self-organization of protein networks (fibrillar structure), which have been confirmed to be of significance in calcification[10, 11].

In reality, as a sophisticated healing of bone, the material should be ultimately integrated into surrounding tissues. Therefore in an experimental study, the material's ability to promote osteointegration needs to be proved. This process involves not only the adsorption of proteins and cellular adherence, but also the

proliferation, migration and differentiation of cells encountered with materials[12]. When damage occurs, local cells can be either removed away or completely destroyed, and cells at the periphery of the area located in one or several cell lines wide can also be disturbed[13]. Therefore, ability of osteoblasts to proliferate and migrate to populate the site is of significant importance. Once the number of osteoblasts present is adequate and they have the tendency to preferentially migrate toward the damaged site, new bone generation, described as mineralization for *in vitro* studies, is expected to occur in a proper microenvironment for successful treatment. Mineralization can be characterized by changes in alkaline phosphatase (ALP) activity during the early stage and accumulation of calcium phosphate during the later stage. Previous reports confirmed that all these behaviors of cells were substrate-dependent[8] and none of them alone was able to comprehensively assess the effect of surface properties on cell response[12]. However, unfortunately the molecular mechanism underneath still remains poorly understood, which is partially caused by the fact that cellular response to biomaterials varies when different substrate systems are employed[6, 14]. To solve this problem, increasing attention has been paid to substrate properties, specially the modification of substrate surface chemistry.

When osteoblasts come into contact with a certain substrate, surface chemistry (e.g. wettability or hydrophilicity) is always involved in regulating cellular response. For instance, Lenhert *et al.* applied plasma treatment to their patterned

polystyrene surfaces to make them more hydrophilic[15] before cell culture experiments, because their primary test showed that without plasma treatment cells tended to detach from the surfaces after fixation and staining procedure and thus resulted in inhomogeneous cell densities[8]. Causa *et al.* found when the volume fraction of their hydroxyapatite (Hap, main inorganic minerals in bone) addition increased above 13 vol%, the distribution of Hap particles became inhomogeneous in their hybrid scaffold and the porous surface structure was destroyed by the increasing accumulation of Hap, which changed the surface composition and resulted in differences in ALP activity[6]. However, in order to indentify effects caused, at least mainly, by surface chemistry, better experiment design is needed to exclude apparent differences in other surface properties, such as roughness and stiffness. One way is to format a patterned surface with different chemistry in adjacent regions. Work of Thomas *et al.* published in 1997 showed such kind of a patterned surface covered by dimethyldichlorosilane (DMS) and N-(2-aminoethyl)-3-aminopropyl-trimethoxysilane (EDS) alternatively with the help of gradual removal of photoresist. DMS/EDS-patterned surfaces provided convenience for *in situ* observation of cell spatial distribution on an alternative hydrophobic/hydrophilic surface[16]. Another type of design used in abundant studies is to create different terminated-functional groups on substrate surface. Cleaned glass slides and silicon wafers[17], gold-coated glass coverslips[18] and also titanium alloy[19] had been soaked in target polymer solutions to allow the

self-assembly monolayer (SAM) formed on substrate surfaces. Popular terminal groups include -CH_3, -OH and -COOH etc[17-19], which usually contribute to surface hydrophobicity/hydrophilicity discrepancies but without any apparent effects on either roughness or stiffness. However, the diversity of experimental systems still fails to provide a reliable indication of osteoblast response when surface wettability/hydrophilicity is known.

In order to obtain a semi-quantitative relationship between surface wettability and osteoblast behavior, in my work, low-e microscope (MirrIR) slides are employed as base substrate, the infrared reflective Ag/SnO_2 coating of which provides the feasibility of non-invasive measurements of the cellular function using vibrational spectroscopy[20]. In addition, its superb optical quality permits the *in situ* observation of both cell migration and fluorescent staining. Negatively charged SPS was chosen as a standard coating material because SPS has been shown to be a critical surface for inducing a fibrillar network of osteoblast extracellular matrix proteins. This ECM network is needed for subsequent calcification of the mineralization stage[21], and the fabrication of SPS coating is easy and stable[10]. But one challenge is that multiple differences coexist between the surface properties of SPS-coated and uncoated slides, such as chemical component and surface charge. To simplify and extend our explanation of how each individual factor listed above influences osteoblast behavior, tissue culture plates (TC) and microscope glass coverslips (glass) are introduced as

controls. TC is a standard substrate for *in vitro* cell culture currently with a polystyrene coating that is plasma etched for better cell adherence. Glass had been used in tissue culture practices prior to TC and is similar to MirrIR slides without the IR-reflective coating. In addition, contact angle measurement showed that TC and glass have similar hydrophilicity as that of SPS-coated and uncoated MirrIR slides, respectively. Roughness of each substrate qualified using Scanning Probe Microscope (SPM) implies that all the substrates turn out to have a roughness of the comparable magnitude, though glass is slightly smoother than the others.

Therefore, the goals of my research are to (1) identify effects of surface chemistry on osteoblast proliferation, migration and differentiation, and explore relationship between surface hydrophilicity and osteoblast response; (2) optimize surface chemistry combined with other surface properties, like charge, to realize an optimal osteoblast response; (3) introduce environmental friendly materials, such as chitosan and gelatin, to replace MirrIR based substrates for future applications.

Chapter Two. Materials and Methods

2.1 Substrate Preparation and Characterization

2.1.1 Substrate Preparation

Infrared reflective MirrIR microscope slides (Kevley Technologies, OH) were partitioned into ~10 mm x 10 mm pieces, cleaned with 100% ethyl alcohol, and spin-coated with a thickness of ~40 nm sulfonated polystyrene (SPS) using 8mg/ml solution in dimethylformamide. A separate batch of uncoated MirrIR slides was cleaned with 100% ethyl alcohol prior to use. Microscope cover glasses (Fisher Scientific) were sonicated in methanol for 10 min at room temperature, boiled in freshly mixed ammonia-peroxide solution for 10 min and rinsed with deionized (DI) water prior to use. Tissue culture (TC) dishes were cut from 10cm TC plate (BD Falcon) into ~10mm x 10mm pieces, when necessary.

2.1.2 Water Contact Angle (WCA)

The static contact angles of sessile drops of DI water on TC, SPS/MirrIR, MirrIR and glass were measured using CAM 200 Optical Angle Meter (KSV Instruments Ltd.) in air at room temperature. A drop of 10µl DI water was added

vertically onto the dry surface, contact angles were measured immediately and five drops were averaged as the final contact angle for each substrate.

2.1.3 Scanning Probe Microscope (SPM)

The surface topography was examined using Veeco MultiMode V Liquid Ambient/Scanning Probe Microscope (Veeco Metrology, CA). Measurements were carried out by the tapping-mode procedure, using a silicon cantilever with a spring constant of 12~110 N/m (Nanosensors). All substrates were soaked in 70% ethyl alcohol and rinsed in sterile phosphate-buffered saline (PBS) before measurement to maintain the same conditions as that for cell culture. Height images were compiled and analyzed using the WSxM Scanning Probe Microscope Software (Nanotec Electronica S.L.).

2.2 Fn Adsorption

Plasma Fn (Sigma) powder was dissolved into autoclaved DI water through incubation in 37°C water bath for 1 hour, according to manufacturer's protocol. Sodium dedecyl sulfate polyacrylamide gel electrophoresis (SDS-PAGE) was employed to verify the molecular weight distribution of Fn in solution. To make the acrylamide gel, mixture of 3.75ml fourfold concentrated separating buffer (18.2g Tris base, 2ml 20% SDS per 100ml with pH adjusted to 8.7), 7.75ml DI water, 3.5ml acylamide/bisacrylamide (30:0.08) % in DI water and 0.05ml freshly made 10% amino persulfate was gently wobbled. Plate assembly was cleaned,

dried with 95% ethanol and sealed with Vaseline. Separating gel solution was transferred into after adding 0.05ml TEMED and let polymerized at room temperature for 1hour. To guarantee an even interface, extra DI water was pipette in to top off. Stacking gel, composed of 1.25ml fourfold concentrated stacking buffer (6.05g Tris base, 2ml 20% SDS per 100ml with pH adjusted to 6.8), 3.05ml DI water, 0.67 ml acylamide/bisacrylamide(30:0.08)% in DI water, 0.05ml 10% amino persulfate and 0.05ml TEMED, was added after the aspiration of DI water and let polymerize for 30 minutes with a clean comb to create the separated wells. After polymerization, gel together with glass plates was mounted into a Bio-RAD gel box full of 1x reservoir buffer (1.51g Tris base, 7.2g glycine and 1g SDS per 500ml). Concentrations of Fn solution incubated at 37°C for 0, 1, 36 and 48 hours were measured with nanodrop Spectrophotometer (ND-1000). Four to six measurements for each case were averaged and calculation was done to obtain equal amount of Fn per 10μL of 1:1 dilution with twofold concentrated sampling buffer (20ml glycerol, 13ml 1M Tris-HCl with a pH of 6.8, 20ml 20%SDS, 47ml DI water and 1mg Bromophenol blue). Duplicate was prepared for each group. Gel was first stimulated with a low voltage of 80V for 30min and then run under 110V. When the blue frontiers reached the bottom, gel was released from the plate assembly, stained with Coomassie Blue (1.25g Coomassie Brilliant Blue, 50ml acetic acid, 200ml DI water and 250ml methanol) for 1hour under gentle shaking and destained with a 1:3:6 mixture of acetic acid, methanol and DI water

after several replacement of fresh destain solution until gel appeared to be clear again. Wet gel was scanned and analyzed by comparison with standard ladder.

Prepared substrates were first soaked in 70% ethyl alcohol (in DI water) for 2 hours, then rinsed with PBS and incubated in 20μg/ml Fn diluted with PBS at 37ºC (5% CO_2, humidified) for 1 and 36 hours, respectively. For conformation, substrates were then gently rinsed with PBS and DI water respectively at harvest and dried under mild air flow before AFM measurements, which followed the same procedure of roughness analysis. Substrates after ethyl alcohol soaking and then incubated in PBS for 1 hour were used as controls.

2.3 Cell Culture

Murine pre-osteoblastic cells (MC3T3-E1 subclone 4, ATCC) were maintained at 37°C (5% CO_2, humidified) in α-MEM culture medium supplemented with 10% fetal bovine serum (FBS) (Hyclone, Logan, UT), 100 units/mL penicillin and 100 μg/mL streptomycin (Invitrogen). For differentiation assay, medium was supplemented with 50 μg/mL L-ascorbic acid (Sigma, St. Louis, MO) and 4 mM β-glycerophosphate (Sigma) for up to 28 days. Fresh medium was given every 2 or 3 days.

2.4 Cell Proliferation

Confluent cells were detached from tissue culture plates with 0.05% Trypsin-EDTA (GIBCO) and seeded onto substrates at an initial density of 2,000 cells per cm^2. After incubation of 0 (attaching for 2 hours after seeding), 2, 4, 6 and 8 days, cells were rinsed with phosphate buffered saline (PBS), then fixed with 3.7% formaldehyde (J.T.Baker, USA) and finally stained with 2.5μg/ml 4',6-Diamidino-2-phenylinclole dihydrochloride (DAPI; Sigma) at room temperature. Cells were kept in fresh PBS and processed for fluorescence microscope reading through the 10x objective lens of Olympus IX 51. Cell densities were averaged from three samples for each case.

2.5 Cell Morphology

Morphology of cells harvested at Day 4 was assessed by immunofluorescence staining. Using the same samples after proliferation analysis, cells were permeabilized with 0.4% Triton X-100 (Sigma) in PBS and stained first with a 1:100 dilution of Alexa Fluor 488 phalloidin (AF; Invitrogen) and then with 20μg/ml propidium iodide (PI; Invitrogen), covered at room temperature. Images were recorded through the 40x objective lens with different light filters and a series of images from the same region were composed to exhibit the entire morphology of cells.

Morphology of cells before and after differentiation treatment, for which Day 0 stands for confluent cells without feeding with differentiation medium, while for Day 14, 21 and 28, cells had been feed with differentiation medium for 14, 21 and 28 days respectively before harvest, was assessed using scanning electron microscope (SEM). At harvest, samples were rinsed 2x with PBS, fixed with 2.5% glutaraldehyde in PBS for 15hours at room temperature, dehydrated first from 25%, 50%, 70%, 95% and 100% ethanol in DI water, then from 50% and 100% HMDS in ethanol by soaking in each solution for 10min and finally air dried at room temperature.

2.6 Cell Migration

Migration of cells was evaluated through analyzing the time-lapse movies. Cells were seeded at an initial density of 2,000 cells per cm^2 and let attaching overnight in regular culture medium. For one situation, cells were feed next day with CO_2-independent medium (Invitrogen) supplemented with 10% FBS, 100 units/mL penicillin, 100 μg/mL streptomycin, and 1% L-glutamine (Invitrogen) and the whole culture plate was transferred to a transparent heated stage at 37°C. Time-lapsed images were recorded through the 10x objective lens under the phase contrast mode for up to 2 hours with an interval of 2 minutes or 4~5 hours with an interval of 5 minutes. Nuclei were tracked and migration speed was calculated based on the displacement of each nucleus from adjacent time points. For another

situation, cells were incubated for two days before migration analysis as described before. Triplicates were averaged for the reported migration speed in each case.

2.7 Cell Elongation

Elongation of cells was investigated through the polarized actin skeleton. Cells were seeded at an initial density of 2,000 cells per cm^2. In order to guarantee a stable morphology, cells were incubated for 2 days, after which they were fixed and stained with AF as described in Session 2.4. Fluorescent images were recorded and elongation of F-actin filaments was presented as the length ratio of the longest axis over the shortest perpendicular one (defined as in ref[22]).

2.8 Cell Differentiation

Cells were seeded at an initial density of 50,000 cells per cm^2, and feed with differentiation medium after they became confluent enough to cover at least 90% of the substrate surface. Substrates treated with medium only (without cells) were used as controls.

2.8.1 Early-stage Differentiation

The early stage, during which premature osteoblasts transform into mature osteoblasts, is critical for osteoblast differentiation[4]. ALP activity of cells seeded on TC, SPS/MirrIR, MirrIR and glass were measured as follows. At harvest on day 0 (after cells become confluent), 4, 7 and 11, samples were removed from incubator and rinsed two times with PBS. Fresh lysis buffer

(25mM Tris-HCl with 0.1% Triton X-100 in PBS, PH adjusted to ~7.4) was added. Cells were taken through 3 freeze/thaw cycles and for each cycle they were incubated at 37°C for at least 30min to ensure lysis. Then cells were scraped off samples and cells/lysis buffer was transferred and centrifuged. Supernatants were collected and used for ALP Assay. Working reagent (WR), composed of 6.7mM p-nitrophenyl phosphate, 2.0mM $MgCl_2$ and 0.1M carbonate buffer which brings PH to ~9.8, was prepared one day before and let sit at room temperature for at least 12 hours. In a 96-well plate, 100µL of WR was mixed with 100µL of sample supernatants. The plate was incubated at 37°C and read at 405nm at various time points using a microplate reader (Model EL 800x, Bio-Tek Instruments, Vermont). The absorbance obtained from samples in the absence of cells was subtracted from all data points. Total amount of proteins was investigated using QuantiPro BCA Assay Kit (Sigma) according to the manufacturer's protocol. ALP activity was normalized to the total amounts of proteins and duplicates were averaged for each case.

2.8.2 Late-stage Differentiation

For SPS/MirrIR, MirrIR, glass and TC, Von Kossa staining for minerals was used to study the late-stage differentiation. At harvest on day 0, 14, 21 and 28, samples were rinsed two times with PBS and fixed with 2% formaldehyde at 4°C. After washing with DI water, samples were covered with filtered silver nitrate solution (2g/100ml H_2O) and exposed to ultraviolet light for 20min, then rinsed.

Sodium thiosulfate (5%) was added for 3min and samples were rinsed with DI water. Early time samples were serially dehydrated from 70% to 95% to 100% ethyl alcohol in DI water after fixation, let sit and air dry at room temperature and then rehydrated serially from 100% to 95% to 70% ethyl alcohol in DI water before reading.

2.9 Statistical Analysis

Data for contact angle, surface roughness, cell proliferation, migration, elongation and ALP activity are presented as mean ± standard error. Standard analysis was performed on all results using student's *t*-test and *P* value < 0.05 was considered significant. All data are presented in the order of decreased hydrophobicity.

Chapter Three. Results

3.1 WCA and Substrate Roughness

The WCA measured on substrates are summarized in Figure 2. Uncoated MirrIR slides have a similar WCA to glass, though slightly higher. SPS coating contributes to the increasing hydrophobicity of MirrIR slides, and is more hydrophobic than TC control. The order of hydrophobicity is: SPS/MirrIR > TC > MirrIR > glass. Roughness analysis (Table 1) shows that all substrates have the roughness of the same magnitude. The roughness order is: TC > MirrIR > SPS/MirrIR > glass. Surface topography of bare substrates is displayed in Figure 3. Scratches on TC might be introduced by the fabrication process, because contact mode AFM study using entire TC plates still resulted in images full of scratches (data not shown). Small white dots on glass are probably dust, as higher magnification scanning resulted in smoother surfaces (data not shown).

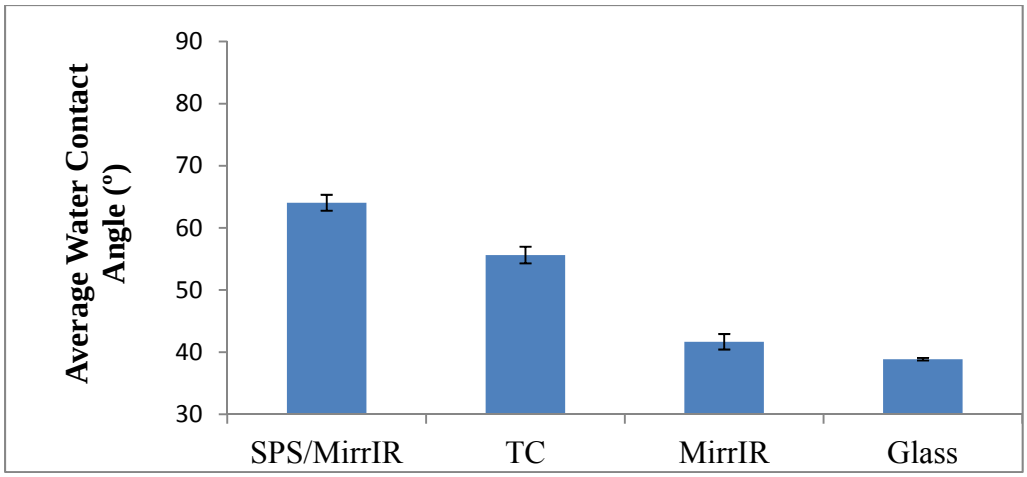

Figure 2 Water Contact angles of SPS-coated MirrIR slides, TC plates, uncoated MirrIR slides and glass, measured at room temperature in air

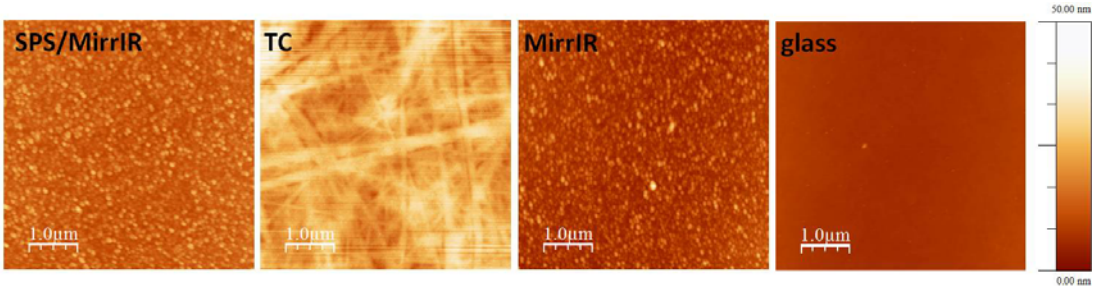

Figure 3 Height images of SPS-coated MirrIR slides, TC plates, uncoated MirrIR slides and glass, measured by the tapping mode AFM in air using a silicon cantilever with a spring constant of 12~110 N/m

Table 1 Surface Roughness

Substrate	RMS roughness (nm)
SPS/MirrIR	2.9
TC	4.5
MirrIR	3.2
glass	0.9

3.2 Fn adsorption

Fn is the main adhesive protein contained in serum[23]. As reported by Steffensen *et. al*[24], fragmentation of Fn could occur as a result of inherent autolytic activities. SDS-PAGE gel confirmed that in our case molecular weight of Fn molecules was mainly above 216kD, which indicated no apparent fragmentation but the entire Fn molecules in solution. The Fn concentration in serum is around 25μg/ml[25], and 10% serum added to our cell culture media contributes to a final concentration of Fn around 2.5μg/ml. We used 20μg/ml to make sure that enough Fn was present for adsorption and feasible detection by AFM.

PBS soaked group was used as a control to exclude effects of possible salt nucleation and crystallization during air-drying process. The incubation time of 36 hours is required for the formation of a Fn matrix in the presence of cells[26] and also for the appearance of dominant interconnected fibrillar structure in the absence of cells[27].

SPM images show that the overall Fn conformation on the surfaces changes as incubation time goes by. On SPS/MirrIR, Fn molecules precipitate to form small particles with apparent non-uniform distribution during the first hour. After incubation of 35 more hours, more and bigger sized grains appear and form connections in between. For TC, aggregate number increases but the connective

structure is less conspicuous. The other phenomenon is that aggregates tend to locate around the scratches. On hydrophilic surfaces of MirrIR and glass, changes are even slighter, with a finer particle size when incubation time increases and further analysis of roughness shows tiny discrepancies between different incubation periods. One possible explanation is that only uniform mono/multilayer of Fn molecules stop on the surfaces but without further extension.

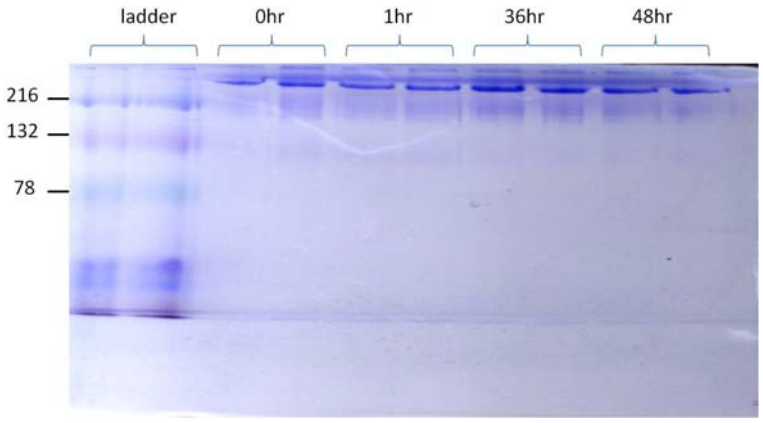

(a)

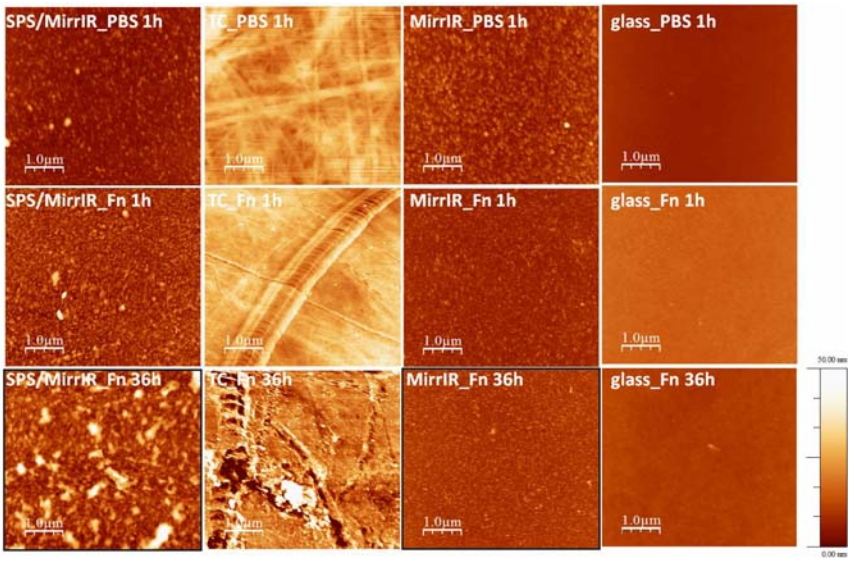

(b)

Figure 4 (a) One-dimensional separation of plasma Fn in autoclaved DI water by SDS-PAGE procedure (see method). The figure shows the protein pattern after stained with Coomassie blue. The following molecular weight was identified through comparison with standard ladder pattern provided by the manufacturer. (b) Height images of Fn adsorption on substrates measured by tapping-mode AFM in air at room temperature using a silicon cantilever with a spring constant of 12~110 N/m (left to right: SPS-coated MirrIR slides, TC plates, MirrIR slides and glass) after incubation of 1(middle) and 36(bottom) hours using 20μg/ml Fn solution in PBS, top is control samples incubated in PBS for 1hour; black border means as incubation goes by surfaces changed with unexpected precipitation whose effects are still poorly understood.

3.3 Cell Proliferation and Morphology

Proliferation of cells on substrates was studied through immunofluorescence staining. Average cell densities at each time point were graphed into Figure 5. Since TC is a favorable substrate known for cell growth, the slower tendency of cell growth on the other substrates thus could be considered as reasonable, without any metastasis unexpected. From the growth curves, it is clear that at the beginning of seeding cells need time to become confluent and after Day 2 difference of growing tendency will show up, especially later than Day 4. Cellular ability of proliferation depends on substrates, for which SPS coating leads to a decrease of proliferation speed on MirrIR slides, which has a similar growing speed to that of glass.

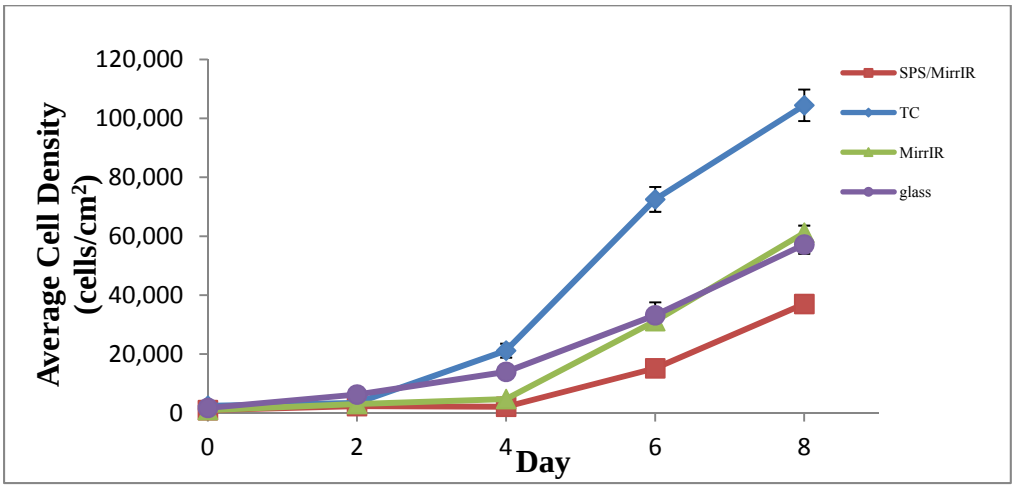

Figure 5 Proliferation of MC3T3-E1osteoblasts on SPS-coated MirrIR slides, TC plates, uncoated MirrIR slides and glass

After proliferation analysis, samples incubated for 4 days were used to assess the morphology, as from the growth curves cells on Day 4 tend to become spread out enough and not very over-crowded, which promises proper space for observing both individual cell spreading and interaction between adjacent cells. Fig. 6 reveals the morphology of cells on TC, SPS/MirrIR, MirrIR and glass, for which blue stains for nuclei, green stains for F-actin filaments and red stains for RNA. Cells attach and spread well on all substrates and the communication between cells can be observed from the connection of F-actin filaments.

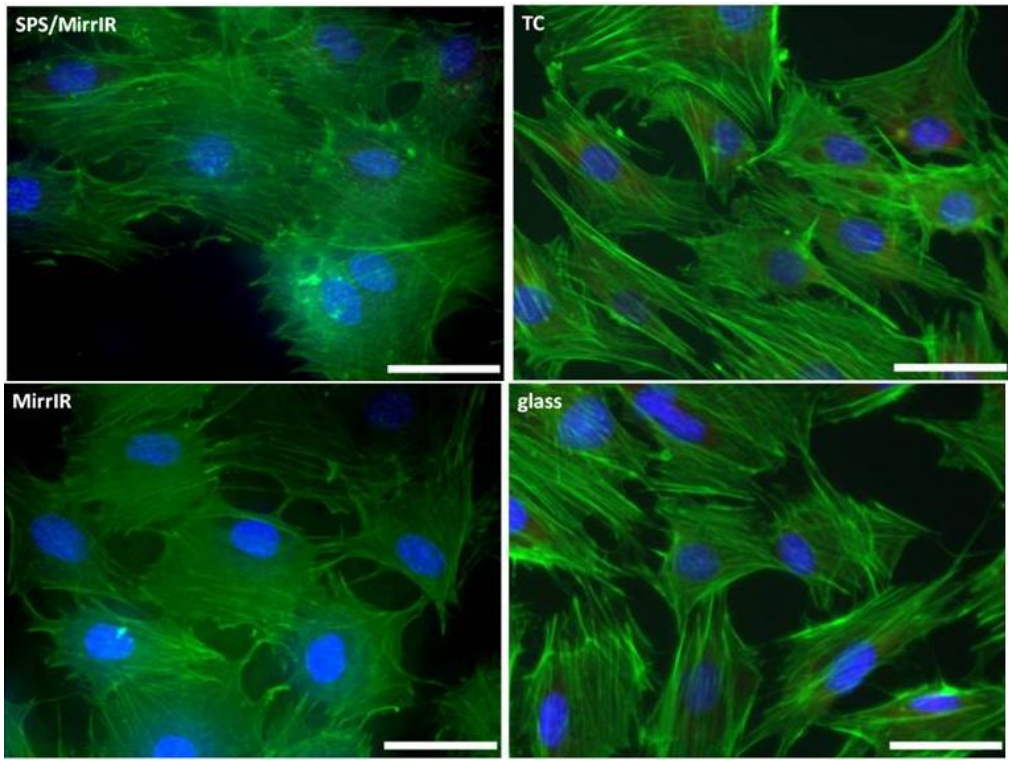

Figure 6 Fluorescence images of MC3T3-E1 osteoblasts incubated for 4 days on SPS-coated MirrIR slides, TC plates, uncoated MirrIR slides and glass. Green is F-actin filaments, blue is nuclei and red is RNA; scale bar = 50μm.

3.4 Cell Migration and Elongation

Cells are capable of movement under appropriate conditions[28]. Nuclei tracking results shows a discrepancy in average displacing speeds of cells monitored by time-lapse movies. After attaching overnight, the fastest speed has been observed in cells migrating on SPS-coated MirrIR slides, while those of MirrIR slides, TC plates and glass have no significant difference in between, regardless of the length of period and interval (Figure 7 (a) and (b)). However, after incubation of 2 days, migration speed on glass exhibits a notable increase while on SPS-coated MirrIR slides cells tend to slow down their locomotion, which thus results in similar migration speeds. Cells sitting on MirrIR slides and glass coverslips maintain their motility. Unfortunately, since cells can functionalize in various ways after they settle down onto a surface, it is really a challenge to attribute such kind of a change to certain cell behavior(s). For instance, after incubation of 2 days, cells become comfortable and they start to divide into new daughter cells. As the time-lapse movie shows, detachment and reattachment happened during division process. Also cells tend to communicate with adjacent cells, during which the signal transmission may delay cell migration.

Additionally, cell polarization is a requirement for cellular movement[2], during which cells have been observed to always protrude their leading edge and also retract their rear to generate forces needed for migration[29], which

contributes to the apparent elongation of cells along certain direction. For our study, the migration is also consistent well with the elongation analysis, though the elongation diversity is not very apparent. (Figure 8) On the other hand, the multiple directional elongation could also be used to prove that none of the substrates used has any apparent regular surface topography, otherwise, patterned topography can contribute to extra alignment and elongation of cells along certain direction.

(a)

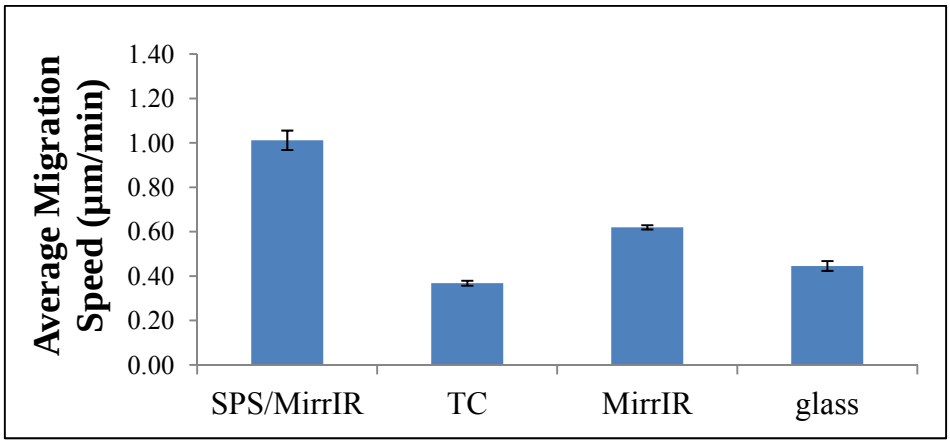

(b)

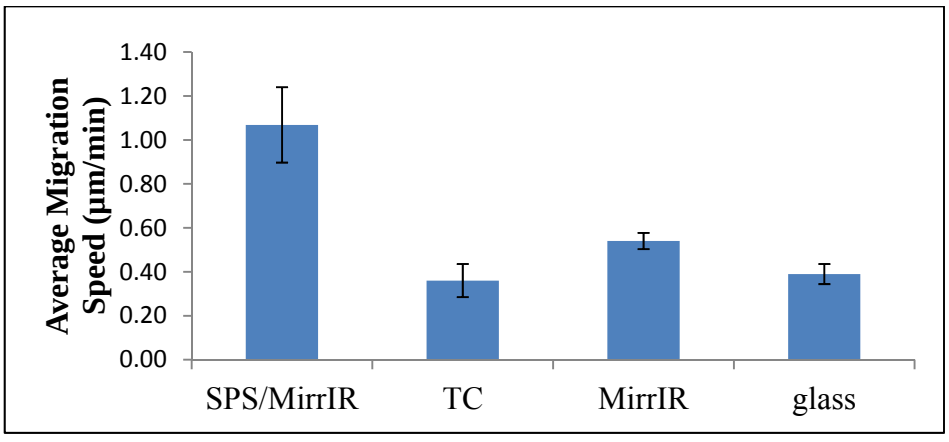

(c)

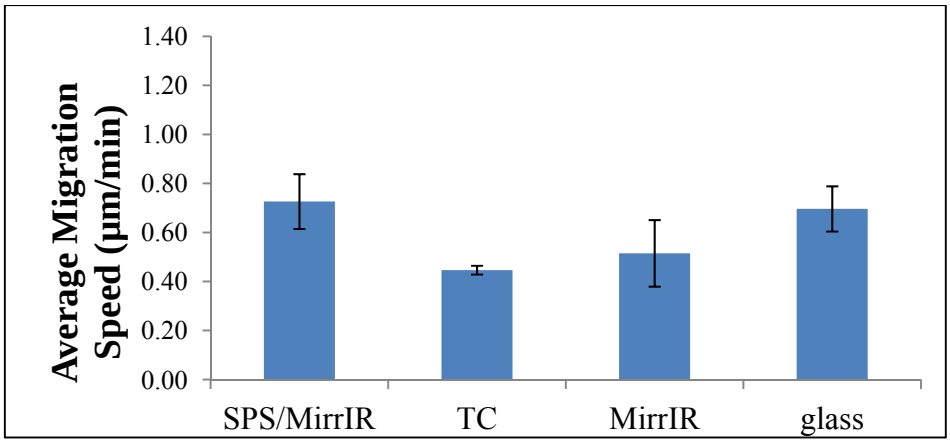

Figure 7 Migration results of MC3T3-E1 osteoblasts cultured on SPS-coated MirrIR slides, TC plates, uncoated MirrIR slides and glass after (a) 18hours, time-lapse movie for up to 2 hours with an interval of 2 minutes (b) 18 hours, time-lapse movie for up to 4~5 hours with an interval of 5 minutes, (c) 2 days, time-lapse movie for up to 2 hours with an interval of 2 minutes

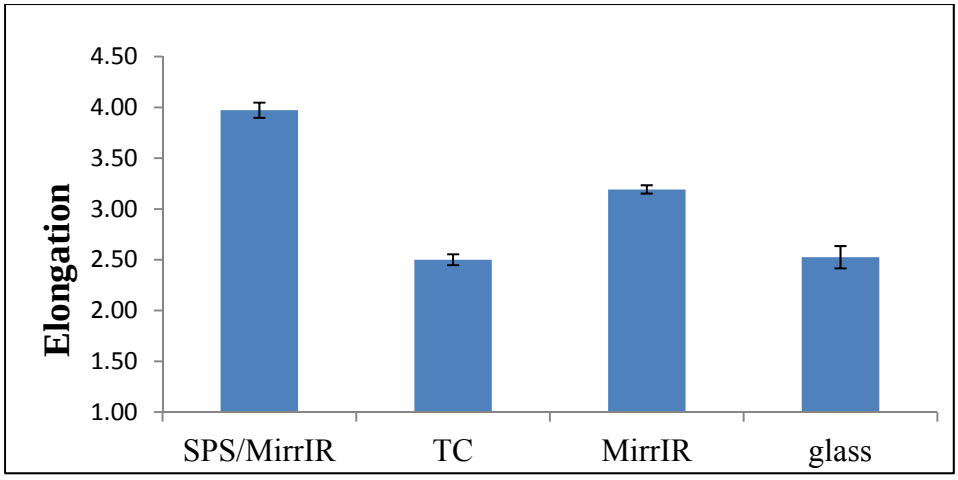

Figure 8 Elongation of MC3T3-E1 osteoblasts on SPS-coated MirrIR slides, TC plates, uncoated MirrIR slides and glass

3.5 Cell Differentiation and Morphology

As a biochemical marker of bone formation secreted by osteoblasts, ALP activity results showed that after feeding with differentiation medium for up to 11 days, OD intensity of ALP activity increased on all substrates. TC exhibited a steady level of ALP after incubation for 4days while for SPS-coated and uncoated MirrIR slides and glass, a significant increasing was found. After then, the amount of ALP for both SPS-coated and uncoated MirrIR slides tends to decrease slightly and maintained at a relatively high level, compared to Day 0. For TC, the increasing appeared more rapidly from Day 4 to Day 7 and then slowed down till Day 11. Glass occupied a steady increasing and the ALP level reached the highest till Day 11.

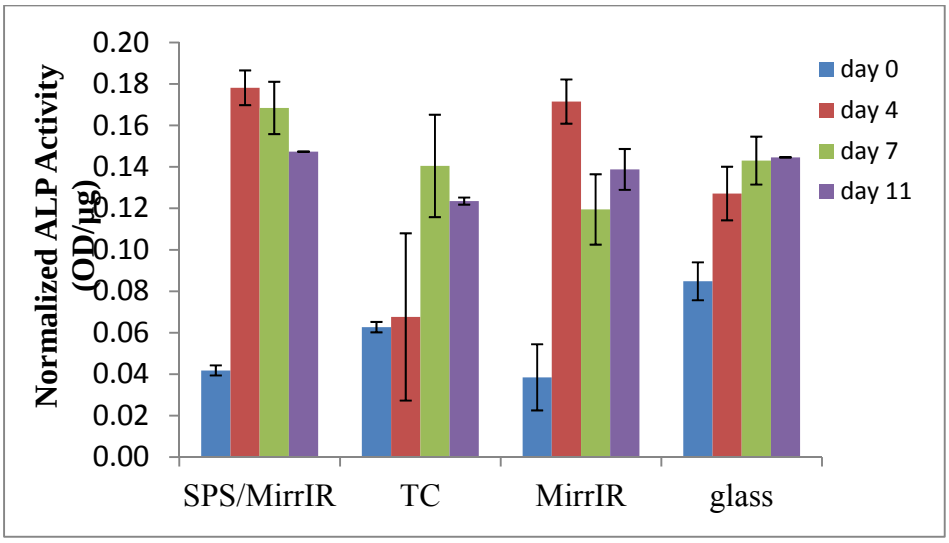

Figure 9 Normalized ALP activity of MC3T3-E1 osteoblasts on SPS-coated MirrIR slides, TC plates, uncoated MirrIR slides and glass, after developing of 120min at 37°C

Von kossa staining in our experiment turns out to be invalid, as even the positive control of TC group[30] have no yellow/brown staining of nodules (data not shown). Since this might be caused by some reason during cell culture process, another improved repeat of the experiment is carried out, which again lead to no positive stain. Based on primary discussion, the staining method might not be suitable for our case, though the reason is still poorly understood. Other element detection method is preferred to replace this part.

Morphology of cells before and after differentiation is assessed. Figure 10 shows that F-actin filaments of cells form less complex connection on SPS-coated and uncoated MirrIR slides than that on TC plates and glass. After feeding with differentiation assay, inconclusive structures appeared on all substrates, which is smaller in size but taller in height than nuclei and they can be stained by both DAPI and PI. Number of these structures tends to decrease when differentiation feeding time increased on TC plates and SPS-uncoated MirrIR slides, while on SPS-coated MirrIR slides and glass, there is no apparent decrease. They could be introduced in by cell differentiation and further identification is needed.

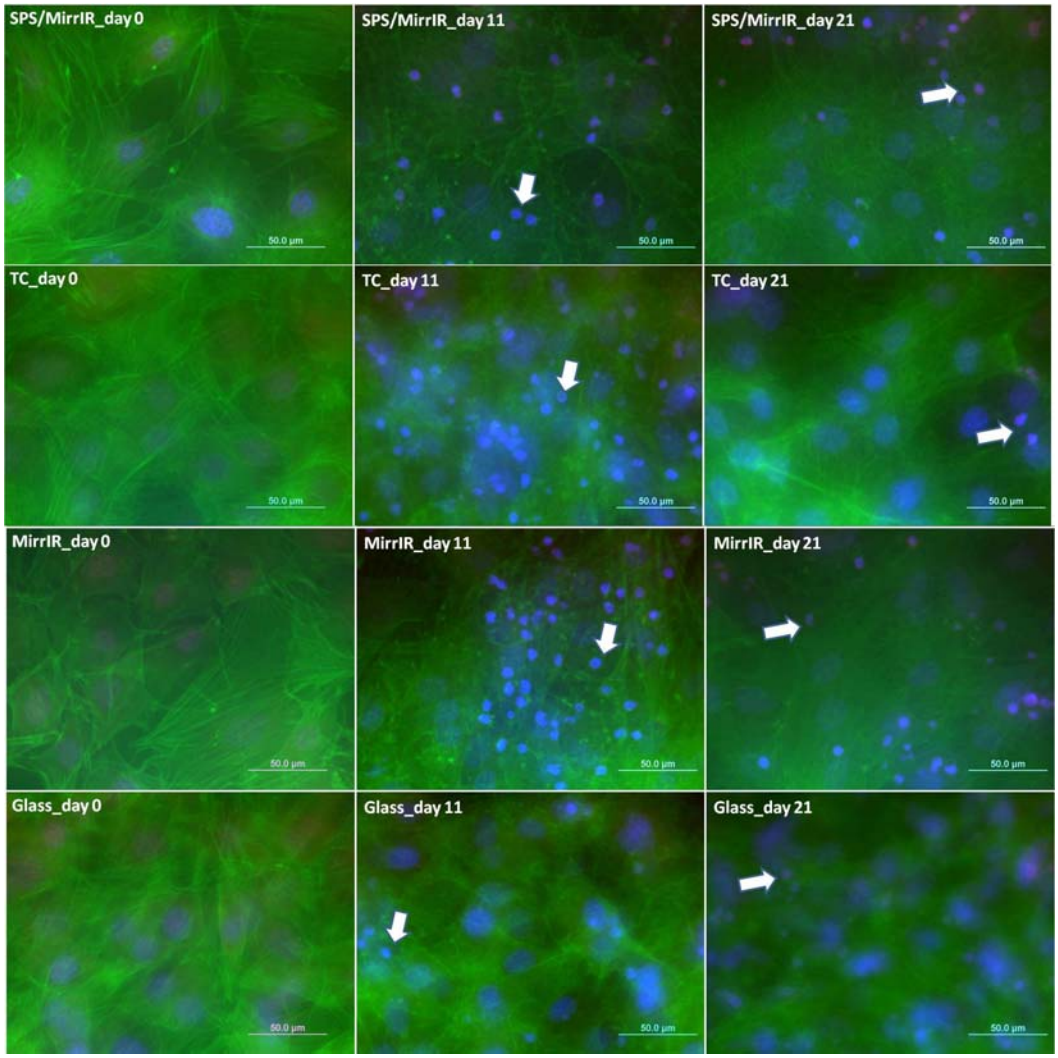

Figure 10 Fluorescence images of MC3T3-E1osteoblasts on TC plates, SPS-coated and uncoated MirrIR slides and glass before (left) and after feeding with differentiation assay for 11 (middle) and 21 (right) days: Green stains for F-actin filaments, blue stains for nuclei and red stains for RNA; scale bar = 50µm; white arrows points to the inconclusive structures formed after feeding with differentiation assay.

Chapter Four. Discussion

Based on the fact that variety of surface chemistry does affect osteoblast behavior in culture, understanding the mechanism of how surface chemistry functionalizes on osteoblasts becomes imperative. As concluded by studies regarding osteoblasts and other cell types, cells, either *in vitro* or *in vivo*, do not encounter a completely bioinert surface. At all times, the material is covered by various components of the fluid in which it is immersed, whether it is body fluid or cell culture media. Which proteins or other components of the medium coat the surface of the material are partially dependent on the surface nature of the material. The potential for proteins to undergo structural rearrangement on the surface itself also plays a significant role. Therefore, the behavior of adsorbed proteins may be related not only to the interaction between the charge of the material and the protein, but also to the protein's potential for change once adsorbed onto the surface. This process is governed by the changes in the hydration of the material surface and the protein, Coulomb interactions between the material and the protein, and structural rearrangements in the adsorbing proteins. As the binding orientation of ions, minerals, water, protein and other

molecules is altered, there is a corresponding change in the cell's attachment to the surface via cell adhesion molecules, resulting in a change in cell shape, and finally the behavior of the cell[12].

In general, osteoblasts on SPS-coated and uncoated MirrIR slides exhibit differences in proliferation, migration and differentiation (at least during the early-stage). Investigation of Fn adsorption revealed different overall protein conformation after incubation for a certain time. As described in previous studies, Fn conformation can be employed to help understand behavior of osteoblast in our experiment. Fn molecules are moderately negatively charged and they tend to have an increased localized negative charge and some positive charge, which depends on the binding interaction between Fn and surface, as the molecules have abundant carboxyl and amino groups. After Fn molecules settle down on the surface, they can extend to some unfolding structure that lead to the alterations in the functional presentation of the particular domains and somehow the hydrophobic cores[31]. Since SPS is also negatively charged, the SPS-coated MirrIR slides most likely have a net negative surface charge, which was presumed to add adsorption and extension of Fn molecules[10].

As extended Fn molecules accumulate on the surface, intermolecular interaction occurs and forms the eventual fibrillar structure[10, 11, 27]. TC surface is hydrophobic and have some irregular microscale scratches, which

change the surface into anisotropic. When Fn molecules come across such a surface, it is possible for them to settle down preferentially to some area and extend to form a stronger binding interaction, such as van der Waals force[32]. Uncoated MirrIR slides and glass are relatively smooth and hydrophilic, and for such kind of substrates, Fn molecules tend to remain their globular structure and form a mono/multi- molecule layers loosely, which is possibly caused by the serious hydration of surface that lead to a strong repelling interaction between Fn molecules and substrate surface[6]. Fn adsorption and their fibrillar structure play a critical role in ECM-mediated cell-material interaction.

Furthermore, Pearlstein *et al.* reported that normal cells are anchorage dependent for growth *in vitro*[31]. Cell cycles can be regulated directly by Fn expression[33] that, in details, G_1 phase has a significant increase in Fn level, S phase shows a constant Fn level and M phase has only little Fn. Cells cannot assemble an Fn matrix, which is necessary for mineralization[11], unless the matrix is in anchored and tension can develop[34]. After Fn assembled into fibrillar structure, those Fn fibrils remain mostly as they have to extend and contract to accommodate movement of cells. Cells have to attach to the fibrils and detach fibrils from themselves alternatively to generate the force needed for migration[26, 35]. And as a late stage of morphogenesis, differentiation can be affect by the early-stage growth stimulation, whose effects have been linked to the expression of a variety of signaling molecules[33]. On SPS-coated MirrIR slides,

Fn from cell culture media can form a fibrillar structure, thus cells can adhere and migrate along after a short attaching period overnight. Expression of cellular Fn and secretion can be regulated differently but beneficially for late differentiation. For uncoated MirrIR slides, TC and glass, cells have to deposit Fn and reorganize them into proper structure, during which up-regulated expression can lead to the acceleration of proliferation but cellular rearrangement of Fn prohibit cell migration or cells may need more time to initiate an apparent movement. This is another reason that why we studied the adsorption of Fn for up to 36h and perhaps a longer attaching time is also helpful before we started our cell migration experiments.

However, unexpected eye-visible spots appeared after incubating SPS-coated and uncoated MirrIR slides for over 1 hour. SEM measurement confirmed the existence and shape of the spots, and AFM analysis showed that both the RMS roughness and average height of the MirrIR slides increased over 10 times after the formation of spots. (data not shown) They might be generated through the chemical reaction between the Ag coating and phosphate ions in the buffer as the precipitates were yellow/brown and insoluble. This problem brings up the necessity of introducing new materials with similar properties of SPS-coated and uncoated MirrIR slides for further exploration of the mechanism involved. Therefore, TC plates and glass coverslips were used to replace SPS-coated and uncoated MirrIR slides, respectively.

Primary AFM study shows differences between RMS roughness of SPS-coated and uncoated MirrIR slides, though not very apparent. However, previous publications concluded that osteoblasts could response differently to substrates based on their roughness[3, 13, 21]. Basically, they proliferated more slowly but were more differentiated on rougher surfaces than smoother ones[12]. Since the sensitivity of osteoblasts to roughness change is still unclear, it is more reliable to diminish this factor as completely as possible before any conclusion about surface chemistry comes out, for which comparison of glass induced even a larger roughness discrepancy. Additionally, quick check of surface electric resistance resulted in that MirrIR slides had a lower electric resistance value than SPS-coated MirrIR slides. As reported in Salehi *et.al*'s work, their nonconductive membrane had a higher capacity of protein adsorption[36]. SPS coating can contribute a net negative charge to SPS-coated MirrIR slides, and this had be proved to help Fn unfolding once adsorbed onto surfaces[27]. All these led to another possibility that the cell culture differences were also influenced by the surface conductivity and surface charge, at least partially. To better explain effect of surface chemistry on osteoblast behaviors mainly, improvement needs to be employed to weaken the diversity of surface electric properties, both surface conductivity and surface charge.

As a support of body, bone occupies advantageous mechanical properties to bear mechanical change from both intrinsic and extrinsic environments, which

contributes to the consideration of suitable stiffness for bone substitutes design. *In vitro* studies using osteoblasts in Hutmacher *et al.*'s work confirmed the normal cellular response of osteoblasts on their three-dimensional (3D) scaffold based on PCL filaments, with a final compressive stiffness vary from ~20MPa to ~40MPa[37]. Causa *et al.* added hydroxyapatite (Hap), main inorganic component of natural bone, to receive an increase in elastic modulus and maximum stress at break and a decrease in strain break of their composite scaffold. Osteoblasts cultured on the composite scaffolds could proliferate to become confluent and differentiate to secrete alkaline phosphate (ALP) marker[38]. In our work, the ~40 nm layer of SPS might have influence on the micro stiffness of MirrIR slides, which need further measurement to be sure. But sulfonation technique had been validated to affect mechanical properties of polymer membrane[39], which added to the imperfection of using TC plates as a comparison.

However, multiple surface characteristics of chemistry, roughness and stiffness, for example, in real life and practical research are always combined in certain way. It is difficult and also unreasonable to separate them from each other, instead, as Kieswetter *et al.* summarized in their review article[12], as the mechanisms of various surface characteristics to be displayed in cell behaviors are similar. More specifically, surface nature leads to conditional adsorption of biomolecules from surrounding fluids and later possibly distinguishing cellular responses. In our case, as concluded by scientists[6] that surface chemistry alone may not be sufficient

explain all kinds of cellular responses, thus instead of trying to separate those properties mentioned above completely for a relative clear influence of single parameter, another choice is to employ new experimental systems with series of surfaces that emphasize one surface properties at a time and finally to combine those influences for an optimal multifunctional applicable design, for example, diamond-based materials and gel fabricated from environmental friendly polymers of gelatin and chitosan/alginate.

Chapter Five. Future Work

To comprehend current results overall and explore molecular mechanism related, future work needs to be centralized on two primary aspects:

5.1 Explanation based on current materials

Based on existing substrates of TC plates, SPS-coated and uncoated MirrIR slides and glass coverslips and current experiment techniques, some more experiment needs to be finished.

5.1.1 Adsorption of Fn

Fn adsorption was assessed in distribution, density and conformation. Current morphology study can only display the overall confirmation change on surfaces. The macroscopic view is not perfect enough in mechanism explanation and microscopic view focusing on molecular level extension is effective to supplement with exact functional binding domains. The other challenge is that after incubation in PBS for longer than 4hrs, SPS-coated and uncoated MirrIR slides tend to be bothered by the unexpected spots, which add to the accuracy decrease of current AFM study. According to other relative studies[11, 40], further study of Fn adsorption can be combined with cell culture. For one thing, our experience showed that when cells were seeded and became confluent on

SPS-coated and uncoated MirrIR slides, no spots would appear when they were kept in PBS. For another, binding interaction between Fn molecules and substrates is weak and the initial characteristics might be disturbed during the air-drying process, so cell behavior could transfer the difference of Fn adsorption into a more stable difference of ECM structure.

5.1.2 Late-stage differentiation study

Von kossa staining didn't work well on all the samples. Since late-stage differentiation can be characterized as the formation of minerals, other techniques that could detect the chemical components of minerals *in situ* are also encouraged to use, such as the EDX in SEM. Bone minerals are hydroxyapatite in nature, which has a Ca/P ratio of ~1.67. Therefore, EDX is hopeful to detect both the existence of Ca and P and also the ratio between them.

5.2 Extension for new materials

As described in the discussion session, convinced explanation of the effect caused by surface chemistry acquires thorough exclusion of extra variables from the comparison group.

5.2.1 Diamond-based Material

Based on our literature study, diamond-based materials are biocompatible both in vivo[41] and in vitro[42]. We chose ultra-nanocrystalline diamond (UNCD) grown on silicon wafer through physical vapor deposition, as kindly provided by Dr. Erik Muller , and their cytocompatibility in our case is displayed as the primary proliferation results in Figure 11. Wettability of UNCD coated and uncoated Si wafer is similar to that of SPS-coated and uncoated MirrIR slides, respectively (Figure 12). And UNCD-coated Si is conductive while bare Si has a higher resistance (data not shown). Furthermore, bundles of physical and chemical treatment can be employed to modify UNCD surface to get a controlled surface roughness and energy[43], which is attractive for our further work.

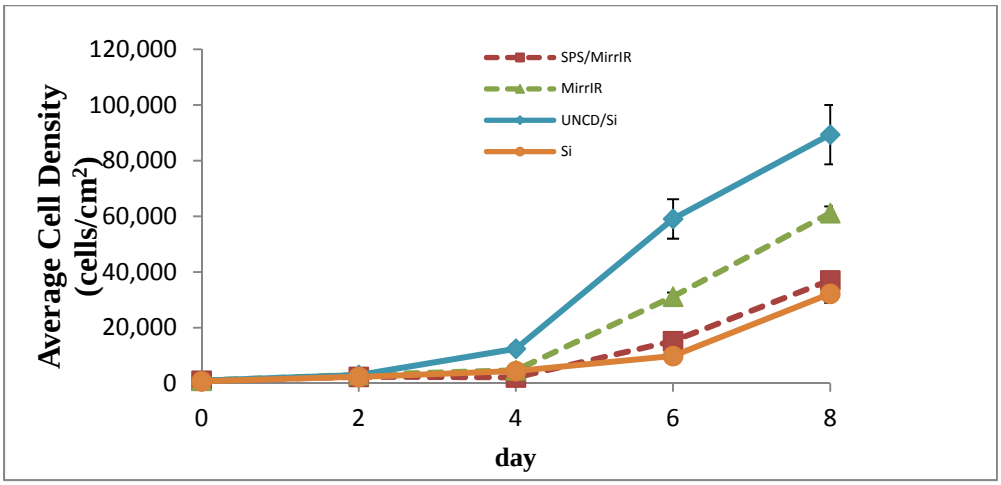

Figure 11 Growth of MC3T3 osteoblast cells on UNCD-coated and uncoated Si wafer, SPS-coated and uncoated MirrIR slides are employed as a control

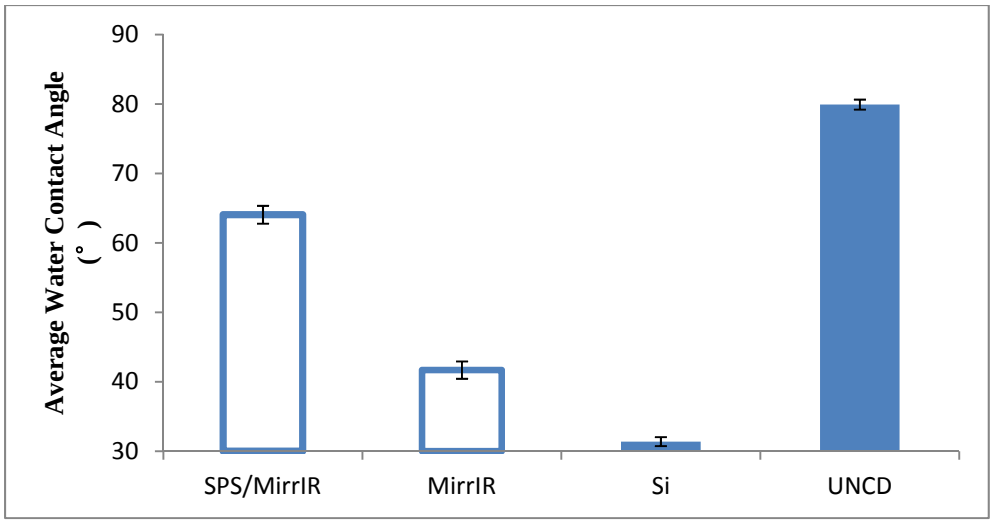

Figure 12 Water contact angle of UNCD-coated and uncoated Si wafer, SPS-coated and uncoated MirrIR slides are employed as a control

5.2.2 Combination of Gelatin and Chitosan/Alginate

Gelatin is an irreversibly hydrolysed form of collagen derived from natural sources such as skin, connective tissue and bones of animals. The film/gel-forming properties of gelatin induce its wide application in classical food, photographic, cosmetic and pharmaceutical industries, such as emulsifiers, foaming agents, colloid stabilizers and biodegradable packaging materials etc[44]. Chitosan is prepared from the alkaline hydrolysis of chitin, which is contained particularly as a horny substance in crab and lobster testae. As a cationic polysaccharide consisting of linear β-1,4-linked GlcN and GlcNAc units (Figure 13(b)), chitosan maintains most unique properties that chitin possesses, such as, antibacterial, antiviral, nontoxic and non-allergic, high radiation resistance, the

capability for the immunological protection against pathogens, biocompatibility and biodegradability[45]. Alginate is a linear copolymer with blocks of (1-4)-linked β-D-mannuronate and α-L-guluronate residues covalently linked together in different sequences (Figure 13(a)). As an anionic polysaccharide extracted from seeweed for commercial product or produced by two bacterial genera, *Pseudomonas* and *Azotobacter* for medical application, alginate can absorb water to form either a viscous solution or gel, and the capability of absorbing can reach 200-300 times to its own weight in water. Additionally, in the acid environment, both alginate salts and alginic acids tend to precipitate to form a low density but viscous gel[46].

Fabrication of 2D[47] and 3D chitosan-gelatin polymer network[47, 48], gelatin and alginate scaffold[49], 3D porous chitosan-alginate scaffold[50] has been reported and their application in cell culture studies has confirmed the non-toxicity and variation of influence depending on the components of scaffolds. For our future experiment, the transparency and thermal stability of gelatin gels offers convenience for *in situ* proliferation, migration and differentiation study. Gel strength can be adjusted through the concentration of gelatin and the amount of cross-linking agents. Addition of chitosan/alginate is expected to change the surface charge of the final gel, which thus can be used to replace MirrIR slides for continuous future study.

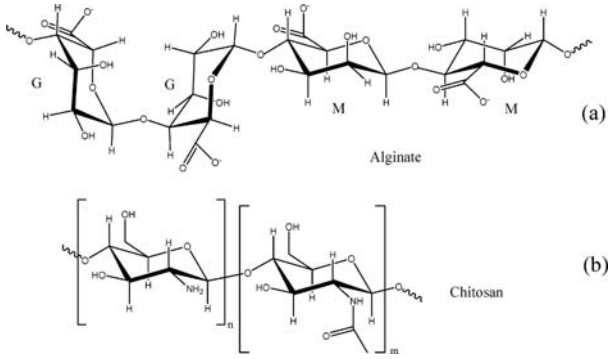

Figure 13 Chemical structures of alginate (deprotonated form) (a) and chitosan (b)[51]

References

[1] Melton LJ, Atkinson EJ, O'Connor MK, O'Fallon WM, Riggs BL. Bone density and fracture risk in men. Journal of Bone and Mineral Research 1998;13:1915.

[2] Langer R, Vacanti JP. TISSUE ENGINEERING. Science 1993;260:920.

[3] Linez-Bataillon P, Monchau F, Bigerelle M, Hildebrand HF. In vitro MC3T3 osteoblast adhesion with respect to surface roughness of Ti6A14V substrates. Biomolecular Engineering 2002;19:133.

[4] Hong D, Chen H-X, Yu H-Q, Liang Y, Wang C, Lian Q-Q, Deng H-T, Ge R-S. Morphological and proteomic analysis of early stage of osteoblast differentiation in osteoblastic progenitor cells. Experimental Cell Research 2010;316:2291.

[5] Burridge K, Fath K, Kelly T, Nuckolls G, Turner C. FOCAL ADHESIONS - TRANSMEMBRANE JUNCTIONS BETWEEN THE EXTRACELLULAR-MATRIX AND THE CYTOSKELETON. Annual Review of Cell Biology 1988;4:487.

[6] Gugutkov D, Altankov G, Rodriguez Hernandez JC, Monleon Pradas M, Salmeron Sanchez M. Fibronectin activity on substrates with controlled -OH density. Journal of Biomedical Materials Research Part A 2010;92A:322.

[7] Llopis-Hernandez V, Rico P, Ballester-Beltran J, Moratal D, Salmeron-Sanchez M. Role of Surface Chemistry in Protein Remodeling at the Cell-Material Interface. Plos One 2011;6.

[8] Altankov G, Groth T. REORGANIZATION OF SUBSTRATUM-BOUND FIBRONECTIN ON HYDROPHILIC AND HYDROPHOBIC MATERIALS IS RELATED TO BIOCOMPATIBILITY. Journal of Materials Science-Materials in Medicine 1994;5:732.

[9] Ruoslahti E, Pierschbacher MD. ARG-GLY-ASP - A VERSATILE CELL RECOGNITION SIGNAL. Cell 1986;44:517.

[10] Subburaman K, Pernodet N, Kwak SY, DiMasi E, Ge S, Zaitsev V, Ba X, Yang NL, Rafailovich M. Templated biomineralization on self-assembled protein

fibers. Proceedings of the National Academy of Sciences of the United States of America 2006;103:14672.

[11] Meng Y, Qin Y-X, DiMasi E, Ba X, Rafailovich M, Pernodet N. Biomineralization of a Self-Assembled Extracellular Matrix for Bone Tissue Engineering. Tissue Engineering Part A 2009;15:355.

[12] Kieswetter K, Schwartz Z, Dean DD, Boyan BD. The role of implant surface characteristics in the healing of bone. Critical Reviews in Oral Biology & Medicine 1996;7:329.

[13] Jones SJ, Boyde A. MIGRATION OF OSTEOBLASTS. Cell and Tissue Research 1977;184:179.

[14] Baugh L, Vogel V. Structural changes of fibronectin adsorbed to model surfaces probed by fluorescence resonance energy transfer. Journal of Biomedical Materials Research Part A 2004;69A:525.

[15] Bhattacharya S, Datta A, Berg JM, Gangopadhyay S. Studies on surface wettability of poly(dimethyl) siloxane (PDMS) and glass under oxygen-plasma treatment and correlation with bond strength. Journal of Microelectromechanical Systems 2005;14:590.

[16] Thomas CH, McFarland CD, Jenkins ML, Rezania A, Steele JG, Healy KE. The role of vitronectin in the attachment and spatial distribution of bone-derived cells on materials with patterned surface chemistry. Journal of Biomedical Materials Research 1997;37:81.

[17] Faucheux N, Schweiss R, Lutzow K, Werner C, Groth T. Self-assembled monolayers with different terminating groups as model substrates for cell adhesion studies. Biomaterials 2004;25:2721.

[18] Keselowsky BG, Collard DM, Garcia AJ. Surface chemistry modulates fibronectin conformation and directs integrin binding and specificity to control cell adhesion. Journal of Biomedical Materials Research Part A 2003;66A:247.

[19] Hunter A, Archer CW, Walker PS, Blunn GW. ATTACHMENT AND PROLIFERATION OF OSTEOBLASTS AND FIBROBLASTS ON BIOMATERIALS FOR ORTHOPEDIC USE. Biomaterials 1995;16:287.

[20] Meade AD, Lyng FM, Knief P, Byrne HJ. Growth substrate induced functional changes elucidated by FTIR and Raman spectroscopy in in-vitro cultured human keratinocytes. Analytical and Bioanalytical Chemistry 2007;387:1717.

[21] Lenhert S, Meier MB, Meyer U, Chi LF, Wiesmann HP. Osteoblast alignment, elongation and migration on grooved polystyrene surfaces patterned by Langmuir-Blodgett lithography. Biomaterials 2005;26:563.

[22] Lamers E, van Horssen R, te Riet J, van Delft FCMJM, Luttge R, Walboomers XF, Jansen JA. THE INFLUENCE OF NANOSCALE TOPOGRAPHICAL CUES ON INITIAL OSTEOBLAST MORPHOLOGY AND MIGRATION. European Cells & Materials 2010;20:329.

[23] Grinnell F. FOCAL ADHESION SITES AND THE REMOVAL OF SUBSTRATUM-BOUND FIBRONECTIN. Journal of Cell Biology 1986;103:2697.

[24] Steffensen B, Chen Z, Pal S, Mikhailova M, Su J, Wang Y, Xu X. Fragmentation of fibronectin by inherent autolytic and matrix metalloproteinase activities. Matrix Biology 2011;30:34.

[25] Hayman EG, Ruoslahti E. DISTRIBUTION OF FETAL BOVINE SERUM FIBRONECTIN AND ENDOGENOUS RAT-CELL FIBRONECTIN IN EXTRACELLULAR MATRIX. Journal of Cell Biology 1979;83:255.

[26] Ohashi T, Kiehart DP, Erickson HP. Dynamics and elasticity of the fibronectin matrix in living cell culture visualized by fibronectin-green fluorescent protein. Proceedings of the National Academy of Sciences of the United States of America 1999;96:2153.

[27] Pernodet N, Rafailovich M, Sokolov J, Xu D, Yang NL, McLeod K. Fibronectin fibrillogenesis on sulfonated polystyrene surfaces. Journal of Biomedical Materials Research Part A 2003;64A:684.

[28] Biname F, Pawlak G, Roux P, Hibner U. What makes cells move: requirements and obstacles for spontaneous cell motility. Molecular Biosystems 2010;6:648.

[29] Anselme K. Osteoblast adhesion on biomaterials. Biomaterials 2000;21:667.

[30] Wang Y-H, Liu Y, Maye P, Rowe DW. Examination of mineralized nodule formation in living osteoblastic cultures using fluorescent dyes. Biotechnology Progress 2006;22:1697.

[31] Pearlstein E, Gold LI, Garciapardo A. FIBRONECTIN - REVIEW OF ITS STRUCTURE AND BIOLOGICAL-ACTIVITY. Molecular and Cellular Biochemistry 1980;29:103.

[32] Anselme K, Linez P, Bigerelle M, Le Maguer D, Le Maguer A, Hardouin P, Hildebrand HF, Iost A, Leroy JM. The relative influence of the topography and chemistry of TiAl6V4 surfaces on osteoblastic cell behaviour. Biomaterials 2000;21:1567.

[33] Williams CM, Engler AJ, Slone RD, Galante LL, Schwarzbauer JE. Fibronectin expression modulates mammary epithelial cell proliferation during acinar differentiation. Cancer Research 2008;68:3185.

[34] Halliday NL, Tomasek JJ. MECHANICAL-PROPERTIES OF THE EXTRACELLULAR-MATRIX INFLUENCE FIBRONECTIN FIBRIL ASSEMBLY IN-VITRO. Experimental Cell Research 1995;217:109.

[35] Lotz MM, Burdsal CA, Erickson HP, McClay DR. CELL-ADHESION TO FIBRONECTIN AND TENASCIN - QUANTITATIVE MEASUREMENTS OF INITIAL BINDING AND SUBSEQUENT STRENGTHENING RESPONSE. Journal of Cell Biology 1989;109:1795.

[36] Salehi E, Madaeni SS. Influence of conductive surface on adsorption behavior of ultrafiltration membrane. Applied Surface Science 2010;256:3010.

[37] Hutmacher DW, Schantz T, Zein I, Ng KW, Teoh SH, Tan KC. Mechanical properties and cell cultural response of polycaprolactone scaffolds designed and fabricated via fused deposition modeling. Journal of Biomedical Materials Research 2001;55:203.

[38] Causa F, Netti PA, Ambrosio L, Ciapetti G, Baldini N, Pagani S, Martini D, Giunti A. Poly-epsilon-caprolactone/hydroxyapatite composites for bone regeneration: in vitro characterization and human osteoblast response. Journal of Biomedical Materials Research Part A 2006;76A:151.

[39] Reyna-Valencia A, Kaliaguine S, Bousmina M. Tensile mechanical properties of sulfonated poly(ether ether ketone) (SPEEK) and BPO4/SPEEK membranes. Journal of Applied Polymer Science 2005;98:2380.

[40] Ba X, Rafailovich M, Meng Y, Pernodet N, Wirick S, Fueredi-Milhofer H, Qin Y-X, DiMasi E. Complementary effects of multi-protein components on biomineralization in vitro. Journal of Structural Biology 2010;170:83.

[41] Yuan Y, Chen Y, Lui J-H, Wang H, Liu Y. Biodistribution and fate of nanodiamonds in vivo. Diamond and Related Materials 2009;18:95.

[42] Schrand AM, Huang H, Carlson C, Schlager JJ, Osawa E, Hussain SM, Dai L. Are diamond nanoparticles cytotoxic? Journal of Physical Chemistry B 2007;111:2.

[43] Schrand AM, Hens SAC, Shenderova OA. Nanodiamond Particles: Properties and Perspectives for Bioapplications. Critical Reviews in Solid State and Materials Sciences 2009;34:18.

[44] Gomez-Guillen MC, Gimenez B, Lopez-Caballero ME, Montero MP. Functional and bioactive properties of collagen and gelatin from alternative sources: A review. Food Hydrocolloids 2011;25:1813.

[45] Prashanth KVH, Tharanathan RN. Chitin/chitosan: modifications and their unlimited application potential - an overview. Trends in Food Science & Technology 2007;18:117.

[46] Yang J-S, Xie Y-J, He W. Research progress on chemical modification of alginate: A review. Carbohydrate Polymers 2011;84:33.

[47] Zhao F, Grayson WL, Ma T, Bunnell B, Lu WW. Effects of hydroxyapatite in 3-D chitosan-gelatin polymer network on human mesenchymal stem cell construct development. Biomaterials 2006;27:1859.

[48] Zhao F, Yin YJ, Lu WW, Leong JC, Zhang WJ, Zhang JY, Zhang MF, Yao KD. Preparation and histological evaluation of biomimetic three-dimensional hydroxyapatite/chitosan-gelatin network composite scaffolds. Biomaterials 2002;23:3227.

[49] Awad HA, Wickham MQ, Leddy HA, Gimble JM, Guilak F. Chondrogenic differentiation of adipose-derived adult stem cells in agarose, alginate, and gelatin scaffolds. Biomaterials 2004;25:3211.

[50] Florczyk SJ, Kim D-J, Wood DL, Zhang M. Influence of processing parameters on pore structure of 3D porous chitosan-alginate polyelectrolyte complex scaffolds. Journal of biomedical materials research. Part A 2011;98:614.

[51] Lawrie G, Keen I, Drew B, Chandler-Temple A, Rintoul L, Fredericks P, Grondahl L. Interactions between alginate and chitosan biopolymers characterized using FTIR and XPS. Biomacromolecules 2007;8:2533.